

CTAO Simulations for Potential PeVatron Candidates

P. Sharma,^{a,c,1} C. Dubos^b S. R. Patel^b and T. Suomijärvi^b

^aThapar Institute of Engineering & Technology, Patiala. India

^bUniversité Paris-Saclay, CNRS/IN2P3,
IJCLab, 91405 Orsay, France

^cUniversité de Strasbourg, CNRS, Observatoire astronomique de Strasbourg, UMR 7550,
F-67000, Strasbourg, France

E-mail: pooja.sharma@thapar.edu, tiina.suomijarvi@ijclab.in2p3.fr

Abstract. This paper reports on the capabilities of the Cherenkov Telescope Array Observatory (CTAO) in detecting high-energy γ -rays that show significant contributions of hadronic origin. We focus on four sources: RX J1713.7-3946, HESS J1731-347, Cassiopeia A, and HAWC J2227+610, which have been previously identified as PeVatron candidates—sources capable of accelerating hadrons to PeV energies. In this study, we perform simulations using Gammapy for each source to obtain flux estimates for CTAO. In case of HAWC J2227+610, we also determined the maximum cut-off energy in the proton distribution detectable by measuring γ -rays with CTAO. To distinguish between fluxes with different proton cut-off energies we used the Test Statistic (TS) method. Additionally, we used the PeVatron Test Statistic (PTS) metric to demonstrate whether CTAO could confirm or exclude SNRs as PeVatron candidates. Through this study, we found that a minimum of 100 hours of observation time is required to detect flux variations with different cut-offs, with the detection limit being ~ 600 TeV. Through the PTS study, SNRs Cassiopeia A, RX J1713.7-3946, and HESS J1731-347 were excluded as PeVatron sources, while HAWC J2227+610 remains inconclusive.

Keywords: cosmic ray experiments, gamma-ray detectors, supernova remnants

¹Corresponding author.

Contents

1	Introduction	1
2	Selected sources	2
2.1	RX J1713.7-3946	2
2.2	Cassiopeia A	2
2.3	HESS J1731-347	2
2.4	HAWC J2227+610	3
3	Simulations	3
3.1	Radiative Models	3
3.2	Source Parameters	3
3.3	Simulations with Gammapy	4
4	Results of Simulation	5
5	Study of different cut-off values	8
5.1	HAWC J2227+610 simulation parameters	8
5.2	Results of the Cut-off Study	9
6	Test for PeVatrons	14
7	Conclusions	15

1 Introduction

The Cosmic Rays (CRs) below the knee (\sim PeV energies) of the CR energy spectrum are expected to have Galactic origins. These high energies are believed to result from the acceleration of cosmic rays (CRs) by shock waves generated in Supernova Remnants (SNRs). It is impossible to observe the origin of CRs directly, as these CRs are charged particles and hence are deflected by the magnetic fields in the Galaxy, causing them to deviate from their path. However, neutral messengers such as γ -rays, produced by CR interactions, open the possibility of pointing to the CR sources. Until now, the SNR G106.3+2.7 (commonly known as HAWC J2227+610) is the only SNR candidate that has shown hadronic emission, due to acceleration of protons, up to PeV energies. However, another scenario, the leptonic one, due to the acceleration of electrons, cannot be ruled out ([10]), ([21]).

To enhance the accuracy of identifying the sources of CRs using γ -ray emissions, it is essential to conduct observations of γ -rays exceeding 10 TeV with a high level of sensitivity, covering a wide energy range, complemented by a good angular resolution. This is made possible by the advent of CTAO, the next-generation γ -ray observatory ([7]). CTAO will be the largest ground-based Imaging Atmospheric Cherenkov Telescope (IACT) observatory. In its Alpha configuration, which includes 14 Medium-Sized Telescope (MST) and 37 Small-Sized Telescope (SST) in the Southern site and 4 Large-Sized Telescope (LST) and 9 MSTs in the Northern site, CTAO will be able to detect γ -ray fluxes with a sensitivity 10x better compared to its predecessors over an energy range of 30 GeV to 200 TeV, covering the entire night sky. The sensitivity of CTAO to detect hadronic PeVatrons, in the context of Galactic

SNRs, has already been studied. In a recent paper ([6]), authors use CTAO Galactic Plane Survey (GPS) simulated data to show that detection from multiple PeVatron SNRs (majorly point sources) can be expected [2]. However, the CTAO GPS has been simulated using 10h exposure and therefore, it is only sensitive to SNRs with a hard proton spectrum ($\Gamma_p = 2$).

This paper aims to investigate potential PeVatron candidates and determine the observational conditions necessary to confirm their PeVatron nature. This paper builds on the previously published multiwavelength (MWL) analysis of Galactic SNRs ([23]), wherein, 9 SNRs were chosen for which sufficient MWL data were available. The observed spectral energy distribution (SED) was then fit with theoretical radiative models; synchrotron, bremsstrahlung, inverse Compton, and pion-decay, using the Naima package ([26]). Through the study, four SNR candidates, Cassiopeia A, RX J1713.7-3946, HAWC J2227+610, and HESS J1731-347, were found to show important hadronic contributions up to the highest energies, making these SNRs potential PeVatron candidates. The sensitivity of the present instruments results in ambiguity regarding the nature of the four sources. This paper aims to study how the detection with CTAO will aid in confirming them as potential PeVatron candidates.

2 Selected sources

In this study, we simulate the flux for previously identified potential PeVatron sources. Basic information about these sources was obtained from the TeVCat database [19] and the literature is summarized in Table 1. These sources have been the focus of extensive prior investigations due to their potential role as cosmic ray accelerators. A concise overview of these studies is provided below.

2.1 RX J1713.7-3946

Evidence for TeV γ -ray emission from the SNR RX J1713.7-3946 was established by [22]. After that, this SNR has become one of the best-studied young SNRs. A paper by the H.E.S.S. Collaboration ([18]) showed that the broadband spectra ranging from radio to γ -rays could not conclusively decide whether the emission is of leptonic or hadronic nature or a mix of both. Furthermore, simulations for CTAO observations of RX J1713.7-3946 were performed, and they revealed that with the exposure time of 50 hrs, CTAO would be able to identify the dominant γ -ray emission component from the morphology of the SNR ([5]).

2.2 Cassiopeia A

Cassiopeia A is another bright, young shell-type SNR that has been proven to be a site of CR acceleration ([9]). Hadronic emission from a component of the SNR has been found through the MWL studies ([3]). Although there is strong evidence for hadronic acceleration up to the highest energies, due to its low cut-off energy, it is unlikely to be a PeVatron source.

2.3 HESS J1731-347

HESS J1731-347 is a young SNR whose MWL counterparts have been studied greatly since its discovery ([16]). Its proximity to a nearby molecular cloud makes this SNR an interesting object of study ([14]). However, its low proton cut-off energy makes it an unlikely PeVatron candidate.

2.4 HAWC J2227+610

HAWC J2227+610 is currently one of the most promising PeVatron SNR candidates. It has shown γ -ray emission up to more than 100 TeV, with no hint of cut-off in its high-energy spectrum ([10]). Thus, this makes it an interesting target for CTAO. It is expected to be out of the field of view of CTAO South, which has been optimized for the study of high-energy Galactic sources. However, CTAO North can observe it with high sensitivity by ensuring a longer observing time. A recent study ([25]) demonstrates that CTAO, with various layouts and observation durations, can effectively detect the source extension and achieve higher detection significance. However, it concludes that it will not be able to disentangle hadronic emission from the leptonic one.

Source	RA (hh mm ss)	DEC (dd mm ss)	Gal Long (deg)	Gal Lat (deg)	Dist. (kpc)	Spec. Index	Type	Age (yrs)	B (μ G)
Cassiopeia A	23 23 13.8	+58 48 26	111.71	-2.13	3.4	2.3	Shell	340 [8]	400 [17]
HAWC J2227+610	22 27 59	+60 52 37	106.35	2.71	0.8	2.29	Int.	4700–5700 [10]	100 [12]
HESS J1731-347	17 32 03	-34 45 18	353.54	-0.67	3.2	2.32	Shell	2000–6000 [15]	50 [4]
RX J1713.7-3946	17 13 33.6	-39 45 36	347.34	-0.47	1	2.2	Shell	1580–2100 [24]	14 [1]

Table 1. List of the chosen SNRs along with basic information found from TeVcat and literature (Int. refers to SNRs interacting with the surrounding medium).

3 Simulations

3.1 Radiative Models

The primary goal of our simulation is to evaluate CTAO’s ability to observe the considered sources with reduced flux uncertainties across a broad energy range. Since our study focuses on hadronic emission, we have considered protons as the parent particle distribution. We assume the energy distribution of protons, $f_p(E)$, to follow an exponential cut-off power-law (ECPL). The distribution for protons is given below:

$$f_p(E) = A_p \times \left(\frac{E}{E_0}\right)^{\alpha_p} \times \exp(-E/E_{p,cut})^\beta \quad (3.1)$$

with:

- A_p : Amplitude of the proton distribution
- α_p : Proton spectral index
- $E_{p,cut}$: Proton energy cut-off
- β : Cut-off exponent

The reference energy has been set to $E_0 = 1$ TeV.

3.2 Source Parameters

The Table 2 encapsulates the values of the physical parameters derived from fitting the theoretical models to the MWL observations using Naima (for more information, refer to the paper ([23])). These parameters have been used as input parameters for the CTAO flux simulation. The reference energy has been set to $E_0 = 1$ TeV. The parameter $K_{ep} = A_e/A_p$

describes the ratio of electrons with respect to protons at 1 TeV. This allows us to redefine A_p as A . Since π_0 production depends on the density of protons in the surrounding medium N_H and the synchrotron radiation depends on the magnetic field B in the radiating region, we need to add two more parameters to obtain the overall fit. \mathcal{L} represents the MaxLogLikelihood.

parameters	RX J1713	Cass A	HESS J1731	HAWC J2227
$\log_{10}(A)$	$49.90^{+0.02}_{-0.02}$	$47.03^{+0.0002}_{-0.0004}$	$47.28^{+0.007}_{-0.009}$	$47.02^{+0.001}_{-0.001}$
α_e	$1.913^{+0.006}_{-0.007}$	$2.80^{+0.001}_{-0.002}$	$2.02^{+0.02}_{-0.03}$	$1.69^{+0.02}_{-0.03}$
α_p	$2.29^{+0.02}_{-0.01}$	$2.10^{+0.01}_{-0.02}$	$1.64^{+0.04}_{-0.04}$	$1.76^{+0.02}_{-0.03}$
$E_{e,cut}$ (TeV)	$4.06^{+0.03}_{-0.04}$	$8.32^{+0.004}_{-0.004}$	$7.41^{+0.04}_{-0.03}$	$0.69^{+0.004}_{-0.004}$
$E_{p,cut}$ (TeV)	$77.87^{+0.04}_{-0.05}$	$23.40^{+0.01}_{-0.01}$	$20.40^{+0.04}_{-0.06}$	$446.68^{+0.07}_{-0.07}$
B (μG)	$252.87^{+4.91}_{-3.29}$	$960.61^{+60.60}_{-38.10}$	$91.98^{+3.63}_{-4.37}$	$596.94^{+12.97}_{-13.12}$
Kep	$0.0023^{+0.00004}_{-0.0006}$	$0.00160^{+0.00002}_{-0.00001}$	$0.0117^{+0.0005}_{-0.005}$	$0.0047^{+0.0002}_{-0.0004}$
n_H (cm^{-3})	$10.29^{+0.15}_{-0.16}$	$163.21^{+1.43}_{-2.37}$	$45.16^{+2.04}_{-2.16}$	$1.70^{+0.09}_{-0.10}$
\mathcal{L}	-128.37	-7.01	-1461.56	-27.45

Table 2. Parameters obtained from the fit for the four SNRs identified as potential PeVatron candidates.

3.3 Simulations with Gammapy

The basic concept behind flux generation involves, first, simulating datasets using the Gammapy dataset class, which stores information about the events, exposure, and background data. Then an astrophysical model is defined using the model classes in Gammapy. Models provide a mathematical representation of the expected γ -ray emission from the source of interest. The models can be spatial, spectral, or temporal in nature or a combination of all. In this study, we focus only on spectral modeling. Once the models are defined, the Gammapy Maker class is used to generate simulated datasets based on these models. Finally, we use Gammapy Estimators, to quantify the properties of the simulated data such as flux and significance. The Naima package is designed to model the non-thermal radiation emitted from high-energy astrophysical objects. Gammapy provides an interface to access Naima, which allows us to simulate physically motivated fluxes.

For the simulation of the CTAO fluxes, it is necessary to check which radiative models help generate the fluxes that accurately match the present instruments' observations. To do so, SEDs combining the simulated CTAO flux at high energy and observed data at low energy were fit with different combinations of radiative models i.e. synchrotron, bremsstrahlung, inverse Compton, and pion-decay using Naima. The analysis revealed that the flux simulated using only the pion-decay model yielded the lowest maximum log-likelihood value. Furthermore, using the pion-decay model significantly decreases the number of parameters compared to combining other radiative models. Due to these factors, in this study, we have chosen only the pion-decay model for simulating the γ -ray flux.

The observation parameters for simulation are tabulated in table 3:

Parameter	RX J1713.7-3946	Cassiopeia A	HESS J1731-347	HAWC J2227+610
IRF	CTAO South Prod5	CTAO North Prod5	CTAO South Prod5	CTAO North Prod5
Zenith Angle ($^{\circ}$)	20	20	20	20
On-Radius ($^{\circ}$)	0.50	0.08	0.18	0.20
Offset ($^{\circ}$)	0.65	0.50	0.50	0.50
Galactic Longitude ($^{\circ}$)	347.3	111.71	106.58	353.54
Galactic Latitude ($^{\circ}$)	-0.47	-2.13	2.91	-0.67
Distance (kpc)	1.0	3.4	0.8	0.8
Source Type	Extended	Point	Extended	Extended

Table 3. Simulation parameters for the selected sources.

4 Results of Simulation

Figure 1- Figure 2, show the simulated flux using the abovementioned parameters. The flux has been simulated in the energy range of 0.003 - 199 TeV. The orange curve depicts the theoretical pion-decay model, the blue points show the simulated fluxes, and for comparison, the grey points which correspond to the real data are plotted on top. For those simulations where the background counts dominate the flux, we obtain only upper limits. Through the plots, upon comparing the simulated and real data in the plots, we can see that CTAO simulated flux extends to larger energies than the current IACT instruments and has much smaller error bars for just 50 hrs of observations. The difference in flux error, between simulated and real data points, has been tabulated below in Table 4. From these values, we can see that the simulated CTAO data is much more precise compared to the real data, leading to significantly lower flux errors. This improvement in precision could allow for better constraints on the fit parameters.

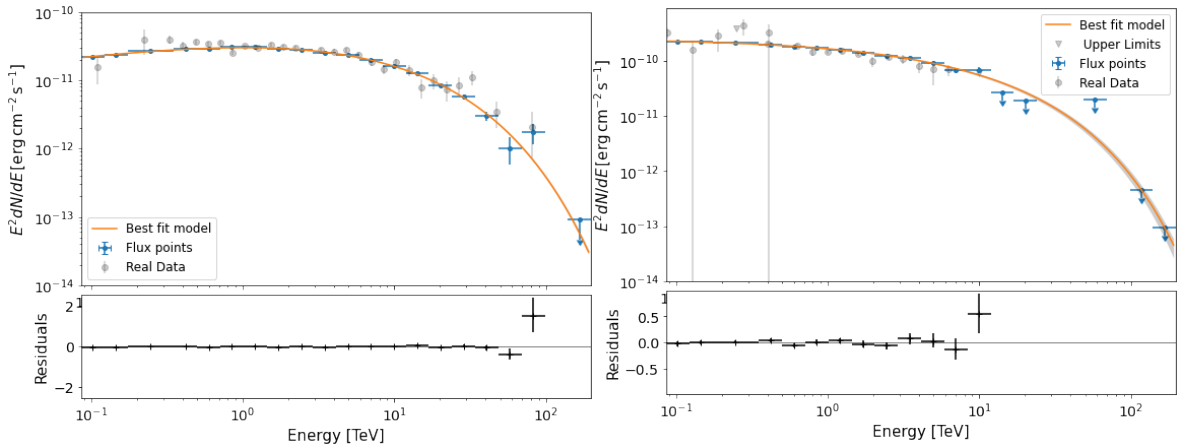


Figure 1. CTAO simulated flux for SNR RX J1713.7-3946 (left) and SNR Cassiopeia A (right), with data points (blue) generated by the pion-decay model (orange) using parameters based on MWL analysis (see text).

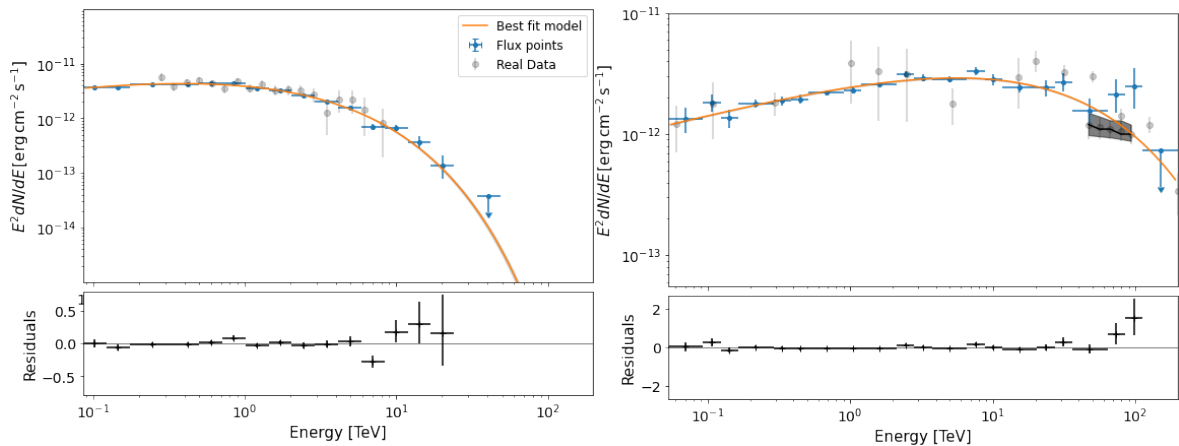


Figure 2. CTAO simulated flux for (left) SNR HESS J1731-347 and (right) SNR HAWC J2227+610, with data points (blue) generated by the pion-decay model (orange) using parameters based on MWL analysis (see text).

Table 4. Comparison of Mean Flux Errors for real data (Err_{RD}) and simulated CTAO data (Err_{SD})

Source	Err_{RD} ($erg\,cm^{-2}\,s^{-1}$)	Err_{SD} ($erg\,cm^{-2}\,s^{-1}$)
RX J1713.7-3946	3.01×10^{-12}	2.76×10^{-13}
Cassiopeia A	7.38×10^{-13}	7.70×10^{-14}
HESS J1731-347	7.38×10^{-13}	6.60×10^{-14}
HAWC J2227+610	6.31×10^{-13}	1.95×10^{-13}

While CTAO will probe very high-energy (VHE) gamma rays, it is crucial to incorporate real lower-energy data available from public archives to gain a more complete understanding of the source and assess how CTAO observations will improve parameter constraints. The real data, as described in [23], is combined with simulated CTAO flux at high energies to create a combined dataset. This combined dataset is then used for SED fitting with Naima, allowing us to evaluate how the inclusion of CTAO data impacts the derived parameters. To avoid statistical biases and instrumental systematics, any real data overlapping with the CTAO energy range has been excluded from the analysis.

Figure 3 shows an example of the fit of the combined dataset using Naima for the SNR RX J1713.7-3946. The solid yellow curve depicts the theoretical synchrotron flux; the green dot-dash curve represents the theoretical flux due to bremsstrahlung radiation; the orange curve with a dotted pattern gives the theoretical flux pertaining to inverse Compton, and the red dashed curve corresponds to emission due to pion-decay. The solid blue curve shows the combined contribution of all these emissions. The real data is shown in black dots and the CTAO simulated flux is shown as cyan dots.

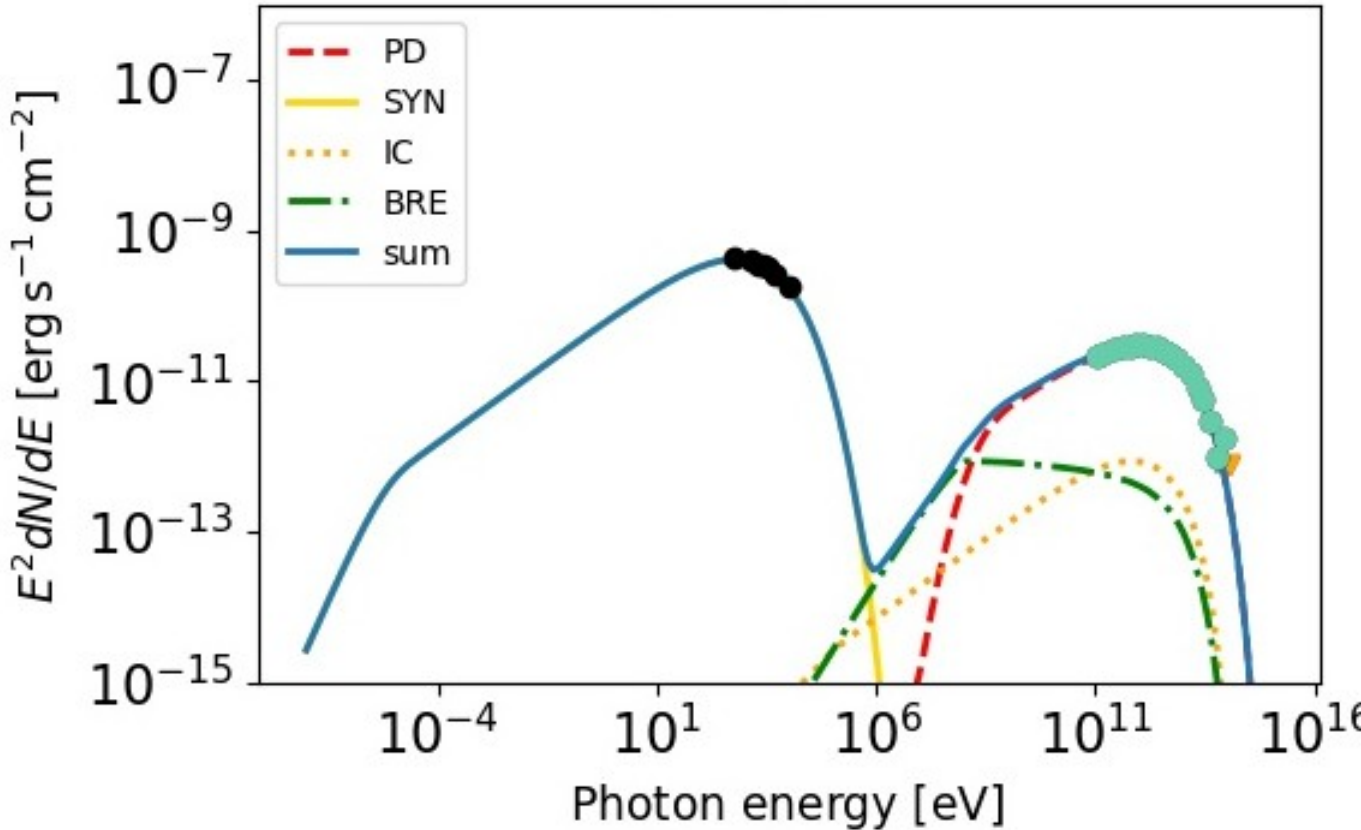


Figure 3. Naima fit result of SNR RX J1713.7-3946 using different theoretical models (see text).

Table 5 compares the proton cut-off energy values and the maximum log-likelihood. The higher $E_{p,cut,CD}$ values suggest that the simulated CTAO data at very high energies helps to push the cut-off energy to higher values. The CTAO’s sensitivity to higher energy photons allows us to better trace the tail of the proton distribution, leading to a more precise determination of the proton cut-off energy values.

Table 5. Maximum likelihood comparison between the real data (RD) and the combined dataset (CD), which consists of real data at low energies and simulated CTAO flux at high energies. The table also includes the proton cut-off energies for both the real and simulated datasets.

Source	$E_{p,cut,RD}$ (TeV)	$E_{p,cut,CD}$ (TeV)	\mathcal{L}_{RD}	\mathcal{L}_{CD}
RX J1713.7-3946	$74.10^{+0.04}_{-0.05}$	$76.7^{+0.02}_{-0.02}$	-37.69	-20.65
Cassiopeia A	$23.40^{+0.01}_{-0.01}$	$27.74^{+0.01}_{-0.01}$	-1461.56	-1254.07
HESS J1731-347	$7.41^{+0.04}_{-0.03}$	$16.22^{+0.03}_{-0.03}$	-7.01	-12.56
HAWC J2227+610	$446.68^{+0.07}_{-0.07}$	$522.73^{+0.06}_{-0.08}$	-27.45	-12.54

The difference between the cut-off energies obtained from fitting real data and those derived after incorporating simulated data can be analyzed to assess the impact of adding high-energy flux points with lower uncertainties on the cut-off value. RX J1713.7-3946 shows a small percentage difference of 3.51% and indicates that the simulated CTAO data closely reproduces the real data. Cassiopeia A and HAWC J2227+610 show a moderate change of

18.55% and 17.03% showing that the simulated data approximates the real data reasonably well but still exhibits notable differences. However, HESS J1731-347 shows a significant difference of 118.89% between the cut-off values of simulated and real data. Since the CTAO simulated data points extend to high energies and have lower flux uncertainties, cut-off values from simulated data are more reliable. Having a more precise cut-off of proton energy values is quite necessary and reflects CTAO’s ability to increase the efficiency of narrowing down the physics of particle acceleration.

We can see that for most sources, the combined dataset provides a much lower log-likelihood than the fit with only the real data (comparison drawn from Table 2). The increased maximum log-likelihood for the SNR HESS J1731-347 may be attributed to minor discrepancies in the flux simulation, which slightly deviates from the model at higher energies. This behaviour may be attributed to the low proton energy cut-off value. Overall, the inclusion of CTAO data at high energies is crucial, as it significantly enhances the constraint on the models, particularly in the multi-TeV domain where current instruments have large uncertainties.

5 Study of different cut-off values

Proton energy cut-off is a critical parameter in hadronic studies as it represents the upper limit of the particle acceleration in astrophysical sources. This in turn reveals important information about the underlying physics, such as shock acceleration efficiency, magnetic field strength, and the age of the accelerating source. Understanding CTAO’s limit to disentangle cut-off values at high energy is crucial to evaluate the ability of CTAO to differentiate between competing leptonic and hadronic processes.

The limited sensitivity of current instruments at the highest energies has, until recently, hindered our ability to precisely constrain the proton cut-off energy. For the source HAWC J2227+610, very-high-energy observations have been provided by HAWC [10] and LHAASO [13], extending the data up to 10^{14} eV. Since the observations extend to higher energies, the simulations can also be extended to these energy ranges, allowing for a more comprehensive comparison. Therefore, this source was selected to evaluate CTAO’s capability to distinguish fluxes corresponding to different proton cut-off energy values.

5.1 HAWC J2227+610 simulation parameters

For the flux simulation, only the pion-decay model was used, for reasons discussed in the earlier section. In Gammapy, the class *Naimaspectralmodel* was used to create a spectral model that convolves an *ExpCutoffPowerLawSpectralModel* proton particle distribution consisting of different values of the proton cut-off energy ($E_{cut,p} = 300, 600, \text{ and } 1000$ TeV) with pion-decay radiation. To define the parameters of the spectral model, we have used the Naima fit results listed in Table 2. Every simulation follows the same procedure, except that we change the proton cut-off energy each time. We performed the flux simulation for three different observing times, 50, 100, and 200 hours observation time to choose the best observing condition. At 200 hrs, we could see a significant increase in the significance with lower error and hence it was chosen for the entire cut-off study.

With the flux now simulated, the next step is to assess the quality of the simulation to determine how closely it matches the input model. To do so, we use the optimizer Minuit ([20]) which can be accessed through Gammapy’s Fit class. We performed a fit between the simulated flux and the respective model used for flux generation. The quality of the fit is

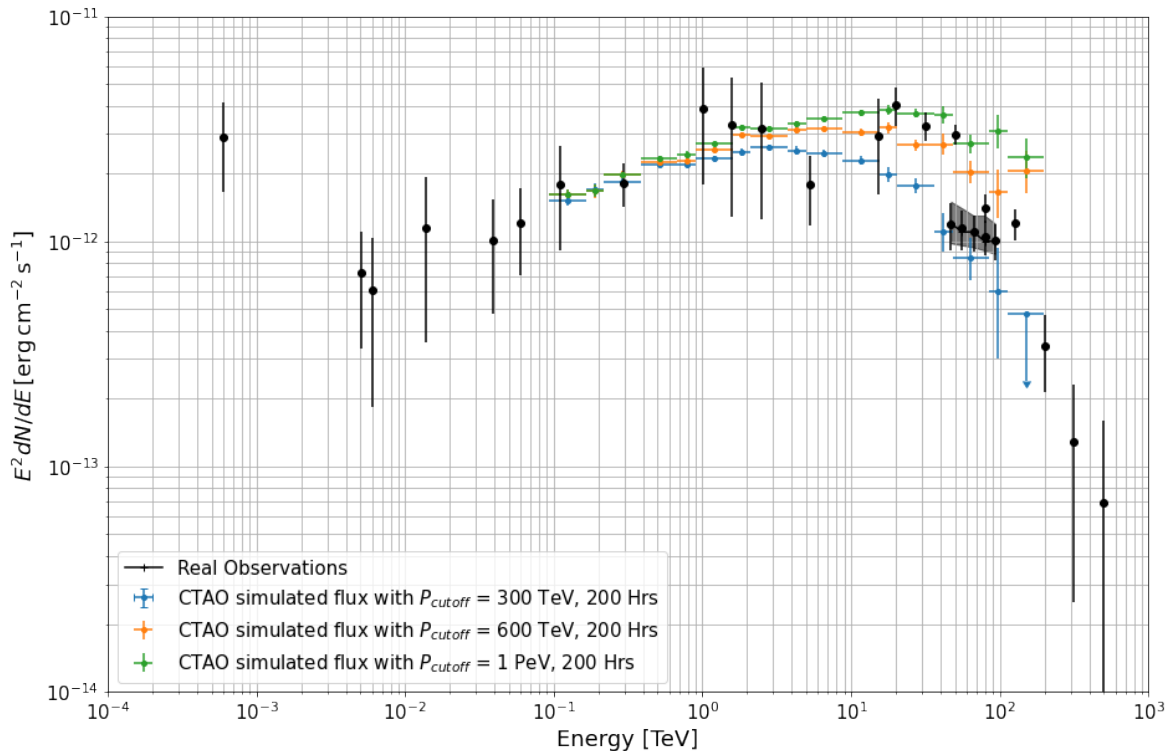


Figure 4. Different simulated CTAO fluxes with varying maximum proton energy. The pion-decay model with $E_{cut,p} = 300, 600,$ and 1000 TeV are represented by blue, orange, and green curves, respectively. The observed data measurements for the source are also shown in black (see text).

given by the Loglikelihood value. Table 6 presents the fitting results of various pion-decay models applied to their corresponding simulated spectra, each with different cut-off values and observation times.

In Figure 4, the observed data taken from [25] have been plotted along with the CTAO fluxes simulated using the pion-decay model with varying proton cut-off energies of 300, 600, and 1000 TeV. These values were chosen as they lie within the minimum and maximum variation of the observed flux extending to the highest energies. From the figure, we can see that CTAO flux points have considerably lower uncertainty compared to the observed fluxes in a similar energy range. Additionally, the fluxes start to differ from one another significantly in the energy range of 1 to ~ 50 TeV. However, due to the limited sensitivity, the flux separation decreases as we go towards higher energies. This shows that sufficiently high statistics around the aforementioned energy range are required to disentangle the fluxes with varying cut-off values.

5.2 Results of the Cut-off Study

To assess CTAO’s capability to differentiate between fluxes with varying proton cut-off energies, we select one of the three simulated datasets and then fit it with all three models with varying proton cut-off energies. When the dataset is fit using the same model used for its generation, it is referred to as the null hypothesis (H0). Then the other models, with different energy cut-off values, become the alternative hypotheses (H1 and H2). This is repeated for

Table 6. The fit results of the simulated CTAO flux of HAWC J2227+610 for a particular proton cut-off energy with its respective pion-decay model. The loglikelihood values (\mathcal{L}) for the observation hrs of 50, 100, and 200 are provided.

Optimizer	Method	Model	\mathcal{L}_{50}	\mathcal{L}_{100}	\mathcal{L}_{200}	Convergence
Minuit	Migrad	PD ₃₀₀	12	8	7	True
Minuit	Migrad	PD ₆₀₀	4	14	12	True
Minuit	Migrad	PD _{PeV}	10	21	22	True

Table 7. The fitting results of various pion-decay models, each corresponding to different proton cut-off energies, against the simulated data for HAWC J2227+610, with the proton energy cut-off value set at 300 TeV.

Optimizer	Method	Model	Δ TS
Minuit	Migrad	H0 _{PD300} -H1 _{PD600}	20
Minuit	Migrad	H0 _{PD300} -H2 _{PDPeV}	55

each simulated data. During the fit, all parameters remain fixed except for the value of the amplitude (A_p) and alpha (α), the exponent of the assumed exponential cut-off power-law distribution.

Figure 5 displays the fit results of both the null and alternative hypotheses models on a fixed simulated CTAO dataset, where the proton energy cut-off is set at 300 TeV. The orange curve represents the PD₃₀₀-model, the blue curve corresponds to the PD₆₀₀-model, and the pink curve is associated with the PD_{PeV}-model. The simulated data points are depicted in dark blue. It is evident that the simulated data align closely with the PD₃₀₀-model, demonstrating the accurate reconstruction of the fluxes based on the model.

To compare the level of agreement of different hypotheses, say, H0 and H1, to a particular data, we make use of the Δ TS-value.

$$\Delta TS = TS_{H1} - TS_{H0} \propto -\ln(L_{H0}/L_{H1}). \quad (1)$$

The fit results have been tabulated in Table 7. Here, the Δ TS value has been calculated using the equation 1. The large Δ TS value suggests that, given the dataset, we can differentiate between the models easily.

Similarly, Figure 6 presents the results of fitting various models with different proton cut-off energy values to a simulated dataset having a proton energy cut-off of 600 TeV. The color scheme remains consistent with the previously discussed representation. It is evident that the simulated data closely aligns with the PD₆₀₀-model, although minor fluctuations are observed at the highest energy levels.

The fit result has been tabulated below in Table 8. The high Δ TS value between different hypotheses suggests that, given the dataset, we can easily differentiate between the models.

In this context, the Δ TS between H0, PD₆₀₀ and H2, PD_{PeV} is relatively small, primarily because of fluctuations in flux at the highest energy levels, rendering both models plausible. This indicates that CTAO’s ability to discern the highest energy fluxes begins to diminish around 600 TeV, establishing it as an upper limit for CTAO’s sensitivity to detect proton cut-off energies.

Finally, to assess the potential of CTAO in detecting a PeVatron source, the dataset containing the simulated data having a proton energy cut-off of 1000 TeV is fit with varying

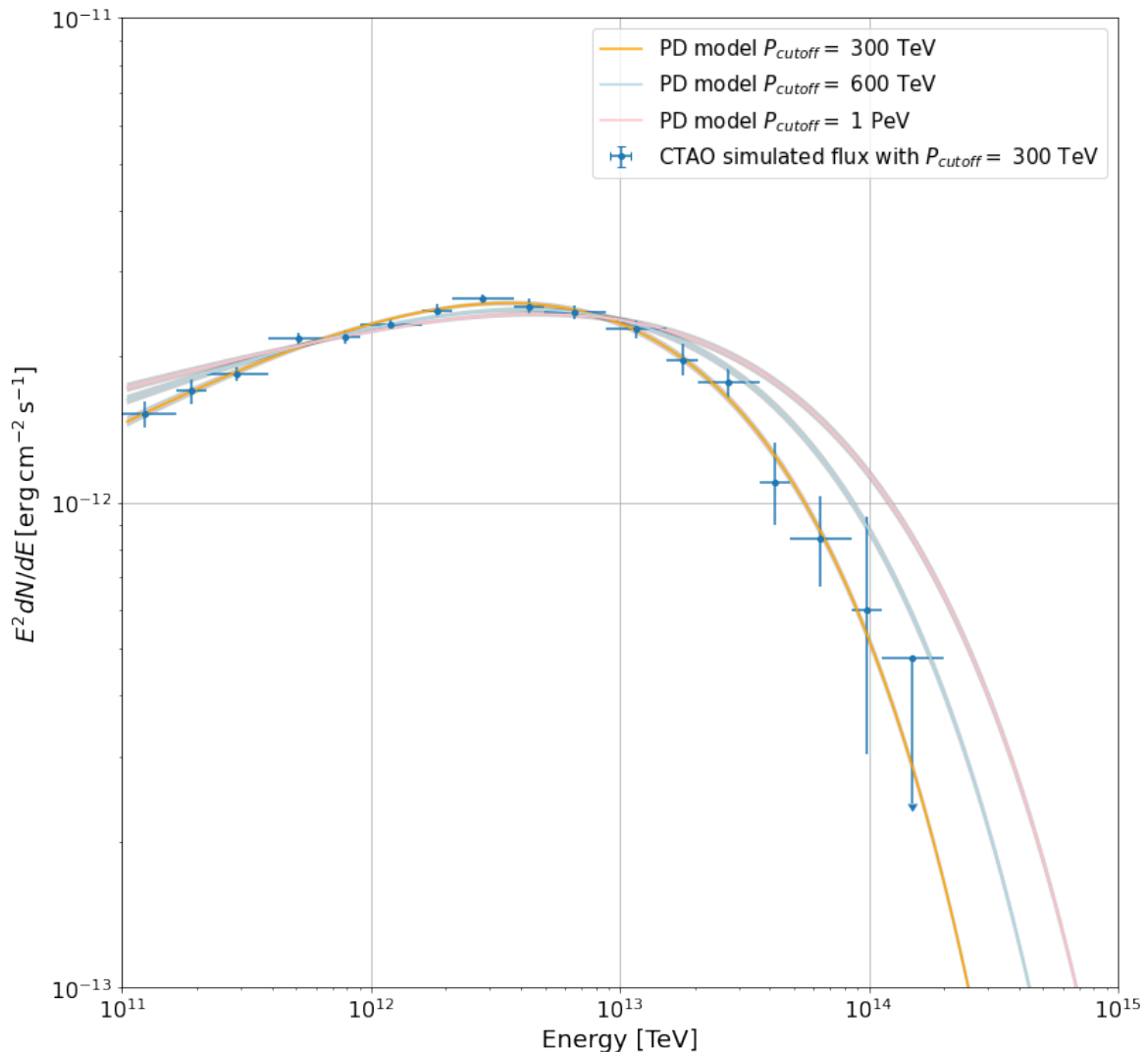


Figure 5. The fit results of the different proton energy cut-off models and the simulated data for HAWC J2227+610 generated using proton energy cut-off value = 300 TeV (see text).

Table 8. The fitting results of various pion-decay models, each corresponding to different proton cut-off energies, against the simulated data for HAWC J2227+610, with the proton energy cut-off value set at 600 TeV.

Optimizer	Method	Model	ΔTS
Minuit	Migrad	$H0_{PD600}-H1_{PD300}$	52
Minuit	Migrad	$H0_{PD600}-H2_{PDPeV}$	-5

pion-decay models. The plot of the fit is shown in Figure 7. The color code is the same as before. Notably, the simulated data closely aligns with the PD_{PeV} -model, indicating a strong agreement. However, fluctuations at the highest energies suggest potential limitations in distinguishing between narrow cut-off energies. Table 10 shows the fit result for the dataset containing flux having a cut-off energy of 1000 TeV with different pion-decay models.

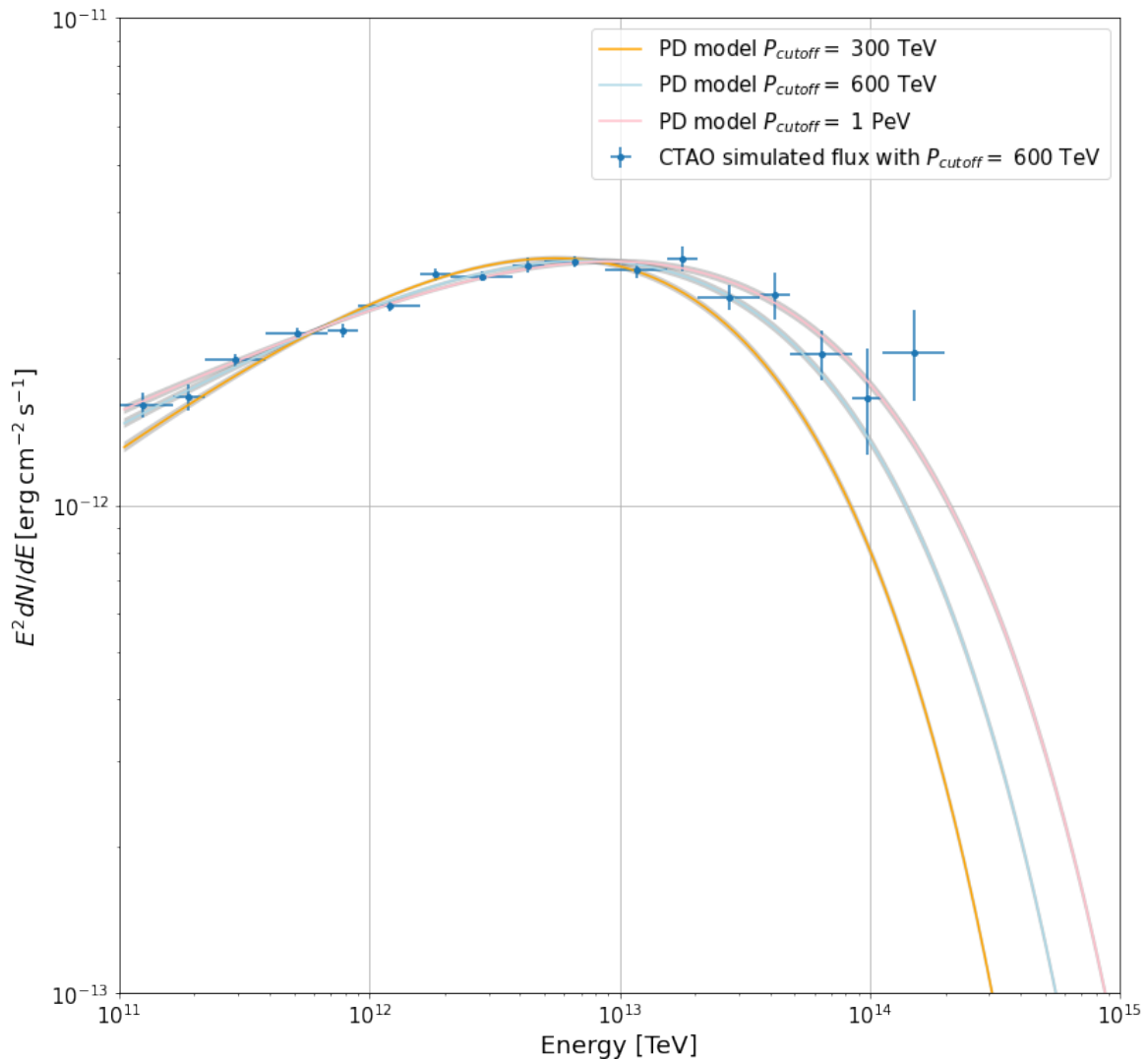


Figure 6. The fit results of the different proton energy cut-off models and the simulated data for HAWC J2227+610 generated using proton energy cut-off value = 600 TeV (see text).

Table 9. The fitting results of various pion-decay models, each corresponding to different proton cut-off energies, against the simulated data for HAWC J2227+610, with the proton energy cut-off value set at 1 PeV.

Optimizer	Method	Model	ΔTS
Minuit	Migrad	$\text{H0}_{PD_{PeV}}\text{-H1}_{PD_{300}}$	128
Minuit	Migrad	$\text{H0}_{PD_{PeV}}\text{-H3}_{PD_{600}}$	30

The high ΔTS values observed for the alternative models relative to the null hypothesis suggest that, with reduced flux uncertainty at high energies, it will be possible to effectively distinguish the flux from PeVatron sources from those with lower cut-off energies.

In conclusion, for datasets simulated with a 300 TeV proton energy cut-off, the model

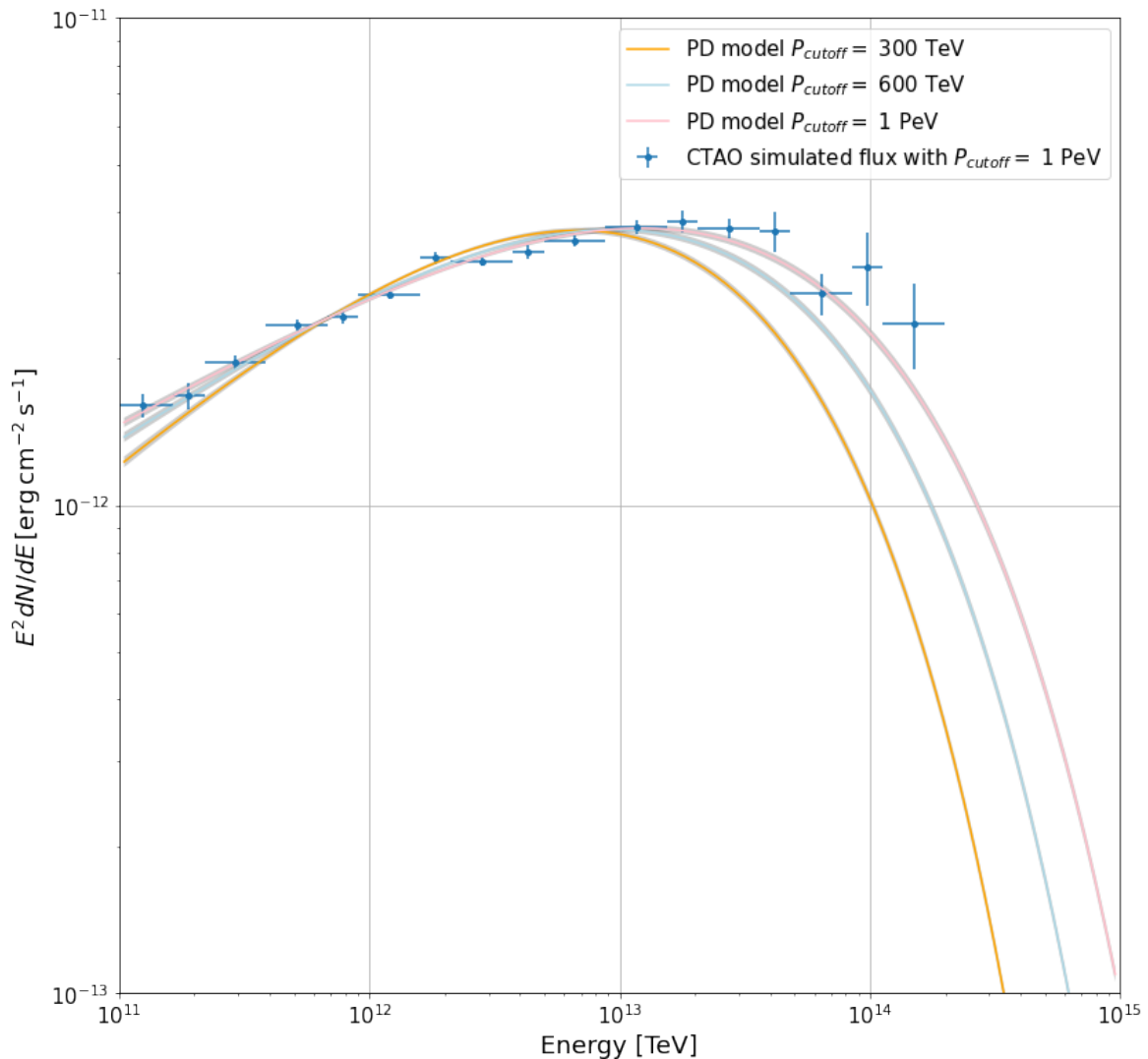


Figure 7. The fit results of the different proton energy cut-off models and the simulated data for HAWC J2227+610 generated using proton energy cut-off value = 1 PeV (see text).

closely matched the data, with high Δ Ts values indicating the ability to differentiate between alternative models effectively. Simulations with a model having proton energy cut-off at 600 TeV, also demonstrated good agreement with the corresponding model, although flux separation diminished at the highest energies, reflecting the limitations of CTAO sensitivity in this range. For PeVatron sources with a proton energy cut-off at 1000 TeV, the simulated data aligned well with the PeV model, with high Δ Ts values when compared to models with lower cut-off values. This indicates that CTAO can effectively identify PeVatron sources within its sensitivity range. However, this ability may be influenced by various factors, such as atmospheric conditions, intrinsic characteristics of the source, and the surrounding environment of the source. The observation time of 200 hrs provided the best Δ Ts values, however, a trade-off between sensitivity and long observing time must be made. While, 50 hrs would be too low to differentiate between different cut-off values, at 100 hrs we begin to reach the

Table 10. The PTS and significance results for the four potential PeVatron candidates.

Source	PTS	S_{PTS}	PeVatron
RX J1713.7-3946	2266	-48	No
Cassiopeia A	684	-26	No
HESS J1731-347	100	-10	No
HAWC J2227+610	4	-2	No

sensitivity required for efficient disentangling of different cut-off values. For sources such as HAWC J2227+610 which show promising characteristics for being a PeVatron source, such long dedicated observing times could be chosen.

6 Test for PeVatrons

The PeVatron Test Statistic (PTS) provides a new approach to detecting spectral signatures of PeVatrons ([11]) and has been used as a second method to estimate the sensitivity of CTAO to detect PeVatrons. To perform the PTS test, two models need to be defined, one with the proton cut-off energy set corresponding to the data and the other with the proton cut-off energy fixed to 1 PeV. These two models are then fit to the simulated data of the 4 SNRs. Using the fit results, one can obtain the total statistic value, which can then be used to calculate the PTS and its statistical significance (S_{PTS}).

PTS is defined as a likelihood ratio test for the deviation of the proton energy cut-off $E_{cut,p}$ from 1 PeV:

$$PTS = -2 \ln \frac{\hat{L}(E_{cut,p} = 1 \text{ PeV}, \boldsymbol{\theta} | \mathcal{D})}{\hat{L}(E_{cut,p}, \boldsymbol{\theta} | \mathcal{D})}, \quad (6.1)$$

and the statistical significance of the PTS is calculated by:

$$S_{PTS} = \text{sign}(E_{cut,p}^* - 1 \text{ PeV}) \sqrt{PTS} \quad (6.2)$$

If S_{PTS} is:

1. $S_{PTS} < -5$, then it is not a PeVatron source (5σ CL)
2. $S_{PTS} \geq 5$, then it is a PeVatron source (5σ CL)
3. $|S_{PTS}| < 5$, data is insufficient to decide whether it is a PeVatron source

N.B. The PTS can only detect a PeVatron source when the true cut-off energy is much larger than 1 PeV.

Using Gammapy, we can fit the simulated dataset with the models specified above. The resulting fit provides the TS value for each model. The difference between the two TS values provides the PTS. The results of the PTS test and its significance have been tabulated in Table 10. The PTS values are highly dependent on the data and hence S_{PTS} values need to be considered with caution. The CTAO simulation has been performed for a wide energy range and has much lower uncertainties due to which it can exclude SNR candidates, Cassiopeia A, RX J1713.7-3946, and HESS J1731-347 to be PeVatrons with a statistical significance of more than 5σ .

The significance value for RX J1713.7-3946 reported in Table 1 of the paper by Ekrem Oğuzhan Angüner et al. [11] is -9.9, indicating a rejection of the PeVatron hypothesis for this source with a significance exceeding 5σ . In this study, we achieve an even stronger rejection, with a significance value of -48. This improvement is attributed to the enhanced sensitivity of CTAO combined with its broader energy coverage. This results in a fivefold improvement in PeVatron rejection. In the same paper, we also find a detailed discussion on the SNR HAWC J2227+610. The significance value stated in Table 3 of the paper when considering only LHAASO observations is consistent with the value of -2 found in this study. Notably, when considering only CTAO simulated data, the significance value for HAWC J2227+610 indicates that the data are insufficient to assess the PeVatron hypothesis. Their analysis highlights that source confusion can lead to inaccurate determination of the total γ -ray spectra, possibly obscuring PeVatron signatures. Additionally, the necessity of using MWL data is also emphasized as it plays an essential role in disentangling leptonic contribution from a hadronic one and has been shown to affect the resulting significance values.

7 Conclusions

This paper attempts to understand the potential of CTAO in searching for PeVatron sources. To do so, we have used open software, Gammapy, (version 0.19) to simulate CTAO flux using radiative models found in Naima library. We focused on four potential PeVatron sources, RX J1713.7-3946, HESS J1731-347, Cassiopeia A, and HAWC J2227+610, which showed significant hadronic contributions ranging up to 100 TeV [23]. For these sources, we first attempted to answer, *How will CTAO observe the flux of these sources?* Through this study, we concluded that CTAO could observe the sources with much lower flux uncertainties, about a factor of ~ 100 , than the present instruments, covering a wide energy range. Naima fit results of the combined dataset of real data with simulated CTAO flux at high energies showed that for most of the chosen candidates, the maximum log-likelihood was reduced significantly. Lastly, by comparing the proton energy cut-off values of real and combined (real at low-energy and CTAO data at high-energy) data, we saw that for some sources the values differed by more than 15%. CTAO's extended coverage at high energies, with lower flux uncertainties, provides more reliable energy cut-off values, and the inclusion of CTAO simulated data significantly varies the value of the fit parameters, thereby improving our understanding of particle acceleration.

Next, to study the capability of CTAO to detect a PeVatron source, we studied *The maximum cut-off energy at which CTAO can effectively distinguish between different fluxes.* Through our study, we found that CTAO could provide flux in the multi-TeV domain, with significantly reduced uncertainty compared to present instruments observing in a similar energy range. This can help in providing better constraints on the source spectral characteristics. We found that a minimum of 100 hrs of observation is required to become sensitive to fluxes with different cut-off values. Through the Test Statistic method, we could define the detection limit for the proton cut-off energy of CTAO to be ~ 600 TeV for the studied source. It should be noted that this detection limit depends on several factors such as observation time, systematic uncertainties, and source characteristics.

As a second method, the PTS metric emerges as a comprehensive measure for confirming or excluding whether a γ -ray source is a PeVatron. With a statistical significance of more than 5σ using only CTAO simulated data, we could confirm that the SNRs Cassiopeia A, RX J1713.7-3946, and HESS J1731-347 are not PeVatron candidates. The PTS study of the

SNR HAWC J2227+610 provided inclusive results due to a lack of data, however, we cannot exclude it as a PeVatron source yet. Results highlight the need for employing high angular resolution observations to mitigate source confusion in the quest for PeVatrons. CTAO with its high angular resolution will be very useful in avoiding misleading conclusions due to source confusion. Additionally, adding MWL observations from complementary instruments will be necessary to ascertain the nature of a source. Together with CTAO, data from future observatories, like the ASTRI Mini-array, and SWGO will help to decide whether SNR HAWC J2227+610 is a PeVatron.

From this study, we conclude that to attain better results, it is imperative to extend the flux measurements to higher energies, perform longer observations for selected plausible PeVatron candidates, and combine MWL data. Recent findings from the CTAO Galactic Plane Survey (GPS) study ([2]) suggest that Supernova Remnants (SNRs) will constitute the second most prevalent category of Galactic γ -ray sources detected by CTAO, following Pulsar Wind Nebulae (PWNe). With CTAO, we stand to significantly enhance our understanding of SNRs as powerful particle accelerators, as the number of detected SNRs is expected to double. Moreover, CTAO will provide information about SNRs with extended geometries, encompassing distances of up to 20 kiloparsecs and fluxes as low as approximately 10^{-14} photons $\text{cm}^{-2} \text{s}^{-1}$. This promising outlook raises the possibility of CTAO substantiating or refuting the hypothesis of SNRs as potential PeVatron candidates.

Acknowledgements

We gratefully acknowledge financial support from the agencies and organizations listed here: http://www.cta-observatory.org/consortium_acknowledgments.

This research has used the instrument response functions provided by the Cherenkov Telescope Array Observatory, & Cherenkov Telescope Array Consortium. (2021). CTAO Instrument Response Functions - prod5 version v0.1 (v0.1) [Data set]. Zenodo. <https://doi.org/10.5281/zenodo.5499840>

References

- [1] H Abdalla, A Abramowski, F Aharonian, F Ait Benkhali, AG Akhperjanian, Tom Andersson, EO Angüner, M Arrieta, P Aubert, M Backes, et al. Hess observations of rx j1713. 7- 3946 with improved angular and spectral resolution: Evidence for gamma-ray emission extending beyond the x-ray emitting shell. *Astronomy & Astrophysics*, 612:A6, 2018.
- [2] S Abe, J Abhir, A Abhishek, F Acero, A Acharyya, R Adam, A Aguasca-Cabot, I Agudo, A Aguirre-Santaella, J Alfaro, et al. Prospects for a survey of the galactic plane with the cherenkov telescope array. *Journal of Cosmology and Astroparticle Physics*, 2024(10):081, 2024.
- [3] A. U. Abeysekara and et al. Evidence for proton acceleration up to tev energies based on veritas and fermi-lat observations of the cas a snr. *The Astrophysical Journal*, 894(1):51, may 2020.
- [4] A Abramowski, Fabio Acero, F Aharonian, AG Akhperjanian, G Anton, Agnès Balzer, Anna Barnacka, U Barres De Almeida, Yvonne Becherini, J Becker, et al. A new snr with tev shell-type morphology: Hess j1731-347. *Astronomy & Astrophysics*, 531:A81, 2011.
- [5] F. Acero and et al. Prospects for cherenkov telescope array observations of the young supernova remnant rx j1713.7-3946. *The Astrophysical Journal*, 840(2):74, may 2017.
- [6] F. Acero and et al. Sensitivity of the cherenkov telescope array to spectral signatures of hadronic pevatrons with application to galactic supernova remnants. *Astroparticle Physics*, 150:102850, 2023.

- [7] Bannanje Sripathi Acharya and et al. Science with the cherenkov telescope array. *arXiv:1709.07997*, 2017.
- [8] Marcel Andre Agüeros and DA Green. The bulk expansion of the supernova remnant cassiopeia a at 151 mhz. *Monthly Notices of the Royal Astronomical Society*, 305(4):957–965, 1999.
- [9] Aharonian, F. and et al.
- [10] A. Albert, R. Alfaro, C. Alvarez, J. R. Angeles Camacho, J. C. Arteaga-Velázquez, K. P. Arunbabu, D. Avila Rojas, H. A. Ayala Solares, V. Baghmany, E. Belmont-Moreno, and et al. HAWC J2227+610 and Its Association with G106.3+2.7, a New Potential Galactic PeVatron. *The Astrophysical Journal*, 896(2):L29, 06 2020.
- [11] Ekrem Oğuzhan Angüner, Gerrit Spengler, Elena Amato, and Sabrina Casanova. Search for the galactic accelerators of cosmic rays up to the knee with the pevatron test statistic. *Monthly Notices of the Royal Astronomical Society*, 523(3):4097–4112, June 2023.
- [12] Yiwei Bao and Yang Chen. On the hard gamma-ray spectrum of the potential pevatron supernova remnant g106. 3+ 2.7. *The Astrophysical Journal*, 919(1):32, 2021.
- [13] Zhen Cao and Aharonian et al. Ultrahigh-energy photons up to 1.4 petaelectronvolts from 12 γ -ray Galactic sources. *Nature*, 594(7861):33–36, June 2021.
- [14] Yudong Cui and et al. Is the SNR HESS J1731-347 Colliding with Molecular Clouds? *ApJ*, 887(1):47, December 2019.
- [15] Yudong Cui, Ruizhi Yang, Xinbo He, PH Thomas Tam, and Gerd Pühlhofer. Is the snr hess j1731-347 colliding with molecular clouds? *The Astrophysical Journal*, 887(1):47, 2019.
- [16] H. E. S. S. Collaboration. A new SNR with TeV shell-type morphology: HESS J1731-347. *A&A*, 531:A81, July 2011.
- [17] EA Helder and J Vink. Characterizing the nonthermal emission of cassiopeia a. *The Astrophysical Journal*, 686(2):1094, 2008.
- [18] H.E.S.S. Collaboration. H.e.s.s. observations of rx j1713.7-3946 with improved angular and spectral resolution: Evidence for gamma-ray emission extending beyond the x-ray emitting shell. *A&A*, 612:A6, 2018.
- [19] Deirdre Horan and S. Wakely. Tevcat: An online catalog for tev astronomy. 03 2008.
- [20] F. James and M. Roos. Minuit: A System for Function Minimization and Analysis of the Parameter Errors and Correlations. *Comput. Phys. Commun.*, 10:343–367, 1975.
- [21] MAGIC Collaboration. *A&A*, 671:A12, March 2023.
- [22] H. Muraishi and et al. Evidence for tev gamma-ray emission from the shell type snr rxj1713.7-3946, 2000.
- [23] Pooja Sharma, Ziwei Ou, Charles Henry-Cadrot, Coline Dubos, and Tiina Suomijärvi. Multiwavelength analysis of galactic supernova remnants, 2022.
- [24] Naomi Tsuji and Yasunobu Uchiyama. Expansion measurements of supernova remnant rx j1713. 7- 3946. *Publications of the Astronomical Society of Japan*, page psw102, 2016.
- [25] Gaia Verna, Franca Cassol, and Heide Costantini. HAWC J2227+610: a potential PeVatron candidate for the CTA in the northern hemisphere. *PoS*, ICRC2021:904, 2021.
- [26] Victor Zabalza. Naima: a Python package for inference of particle distribution properties from nonthermal spectra . *PoS*, ICRC2015:922, 2016.